Storm, rogue wave, or tsunami origin for megaclast deposits in western Ireland and North Island, New Zealand?

John F. Dewey[a,1] and Paul D. Ryan[b,1]

[a]University College, University of Oxford, Oxford OX1 4BH, United Kingdom; and [b]School of Natural Science, Earth and Ocean Sciences, National University of Ireland Galway, Galway H91 TK33, Ireland

Contributed by John F. Dewey, October 15, 2017 (sent for review July 26, 2017; reviewed by Sarah Boulton and James Goff)

The origins of boulderite deposits are investigated with reference to the present-day foreshore of Annagh Head, NW Ireland, and the Lower Miocene Matheson Formation, New Zealand, to resolve disputes on their origin and to contrast and compare the deposits of tsunamis and storms. Field data indicate that the Matheson Formation, which contains boulders in excess of 140 tonnes, was produced by a 12- to 13-m-high tsunami with a period in the order of 1 h. The origin of the boulders at Annagh Head, which exceed 50 tonnes, is disputed. We combine oceanographic, historical, and field data to argue that this is a cliff-top storm deposit (CTSD). A numerical model for CTSDs is developed which indicates that boulder shape in addition to density and dimensions should be taken into account when applying hydrodynamic equations to such deposits. The model also predicts that the NE Atlantic storms are capable of producing boulderites that, when size alone is considered, cannot be distinguished from tsunamites. We review the characteristics that identify the origins of these two deposits.

megaclast | storm | tsunami

The geological record is replete, perhaps dominated, by instantaneous to short-lived events, at many time and space scales, punctuating long periods of relative stasis (1–3). These convulsive, cataclysmic, or catastrophic events such as bolide impacts, earthquakes, volcanic eruptions and flank collapse, floods, storms, and tsunamis cause rapid changes and, commonly, distinctive stratigraphical signatures, commonly boulderites, that record these paleo events (pal-events) as horizons or time–rock markers (see *Mechanisms of Boulderite Formation* for review). However, when such deposits are encountered in modern deposits or the geological record, their origin is often contentious. In *Mechanisms of Boulderite Formation*, the various origins for boulderite deposits are summarized. We have discarded all but two of these origins (tsunamis and storm deposits) for the western Ireland and New Zealand deposits discussed in this paper. Recent debate (4–8) has centered upon the difficulty of distinguishing tsunamites from cliff-top storm deposits (CTSDs), both of which contain boulders with intermediate axes in excess of 3 m. This study compares and contrasts a CTSD on the present-day coast of western Ireland and a newly identified tsunamite in the lower Miocene of New Zealand, which we believe show features that will aid in the characterization of such deposits elsewhere. We also examine the possible temporal development of such deposits, which are both on rocky shorelines, and are rarely described in the geological record because they are commonly seen in simple cross-section (9). We use the nomenclature of Terry and Goff (10) when describing megaclasts.

The fundamental difference between tsunami and other coast-impinging wind-driven waves is their period, run-up, and height. Tsunamis are shallow water, long period (up to 60 min), long wavelength (110 km), fast [800 kph (kilometers per hour) slowing to 50 kph], in wave trains, over up to several days, as a fast-rising flood or bore that may travel up to 2 km inland followed by a sustained backwash. Wind-driven waves are short period (6–25 s), short wavelength (100–200 m), traveling from 10 kph to 90 kph, with multiple back and forth actions in a short space and brief timeframe. Momentum of laterally displaced water masses may be a contributing factor in increasing speed, plucking power, and run-up for tsunamis generated by earthquakes with a horizontal component of displacement (5), for lateral volcanic megablasts, or by the lateral movement of submarine slide sheets. In storm waves, momentum is always important (1 cubic meter of seawater weighs just over 1 tonne) in throwing walls of water continually at a coastline. In addition to transporting boulders, both tsunamis and storm waves may cause plucking of blocks from solid coastal outcrops. Plucking involves higher energies than transport. The size and shape (oblate or slab-shaped versus prolate or rod-shaped; *Numerical Model*) of boulders influences their mode of transport and arrangement in the resultant boulderite. Prolate boulders are easily rolled, whereas oblate boulders tend to tile and imbricate.

Western Ireland

Boulderite deposits are recorded on the west coast of Ireland that are thought to be either CTSDs (4–6), or the result of a Holocene tsunami (7, 8). Ireland is located on a passive margin with relatively quiet seismicity (11). However, 12 possible tsunami events since 14,860 BP and 10 rogue wave events (defined as at least double the maximum significant wave height) since 1852 have affected this region (12). Therefore, several mechanisms could have produced the boulderite at Annagh Head.

Annagh Head, on the Belmullet peninsula of County Mayo (latitude 54.242°N, longitude −10.104°E, Fig. 1 *A* and *B*), is identified as one of the two sites in western Ireland that have wave-emplaced boulders weighing over 30 tons (7). The deposit comprises isolated

Significance

The origin of boulderite deposits in the geological record is controversial. Many argue that boulders weighing over 30 tonnes characterize tsunamites. We compare and contrast two such deposits with boulders exceeding this weight: a tsunamite from the Miocene of New Zealand and a present-day boulderite at Annagh Head, western Ireland. Combining field, historical, and oceanographic data, we argue that the latter is a cliff-top storm deposit (CTSD). Numerical modeling shows that the weight of a boulder in such CTSDs does not just reflect storm wave height, which can be over 60 m in western Ireland, but is also a function of its shape. We review the characteristics that distinguish these two deposits.

Author contributions: J.F.D. and P.D.R. designed research, performed research, contributed new reagents/analytic tools, analyzed data, and wrote the paper.

Reviewers: S.B., University of Plymouth; and J.G., University of New South Wales.

The authors declare no conflict of interest.

[1]To whom correspondence should be addressed. Email: jfdeweyrocks@gmail.com.

This article contains supporting information online at www.pnas.org/lookup/suppl/doi:10.1073/pnas.1713233114/-/DCSupplemental.

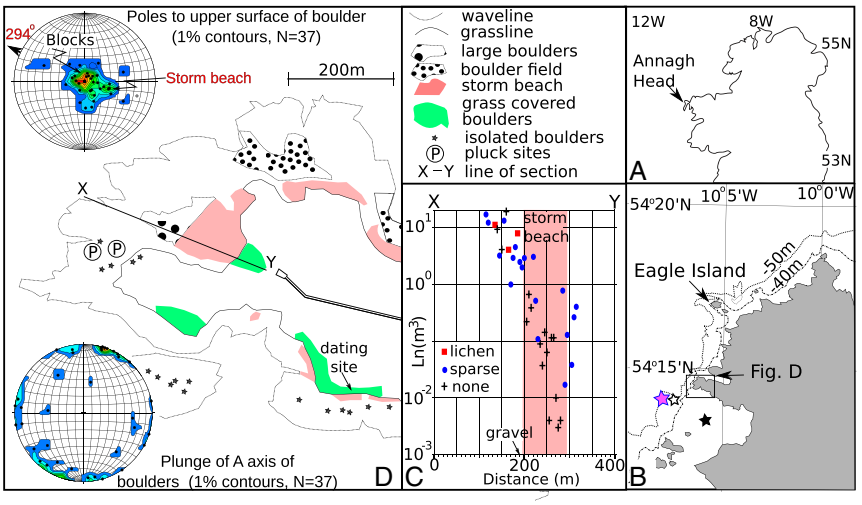

Fig. 1. (*A*) Location map for Annagh Head. (*B*) Map of the north of the Belmullet Peninsula, County Mayo showing 40 m and 50 m bathymetric contours (13), Eagle Island, Wave Rider Belmullet Berth B buoy (large star), ADCP (14) "deep" buoy (small open star), and ADCP "shallow" buoy (small filled star). (*C*) Plot of the distance from the high tide line versus the logarithm$_{10}$(volume) along traverse A-A′ (*D*), which sampled the largest boulder in a 1-m-radius circle every 5 m on a bearing of 115°. The region of the active storm beach is shaded, and the degree of lichen coverage is color coded: black cross for no lichen on the upper surface, blue circles for sparse lichen, and red squares for significant lichen. (*D*) Map of the Annagh Head deposit. (*Insets*) Equal area stereoplots for (*Top*) the orientation of the upper surface and (*Bottom*) the plunge of the long axis of the boulders recorded on the Annagh Head traverse.

boulders lying on a wave-swept rocky foreshore 2 m to 5 m above high tide lying in a glacially excavated shallow trough, facing 295°, bounded to the north and south by rocky headlands 10 m and 25 m above sea level, respectively (Fig. 1*D*). Heights were derived from the Shuttle Radar Topographic Mission 1 arc-second database (data available from the US Geological Survey). Boulders in excess of 30 tonnes do not occur on other rocky shores to both the south and north sides of the peninsula, although both contain significant storm beaches and peat-covered boulder deposits, which have been dated a >4000 B.P. (10). The bedrock comprises calc-alkaline orthogneisses of the Annagh Gneiss Division of Paleoproterozoic age (15), which contains local amphibolitized tholeiitic sheets that were emplaced after gneissification (16).

A traverse was taken along the rock platform, recording the largest boulder found within a 1-m circle every 5 m. The direction of traverse was 115°, parallel with the axis of the glacial trough and orthogonal to the trend of the storm beach bar. The traverse extended 315 m from the low tide line (shoreline) to the point behind the storm beach where no "fresh" (not overgrown by grass) boulders were visible. The following parameters were recorded

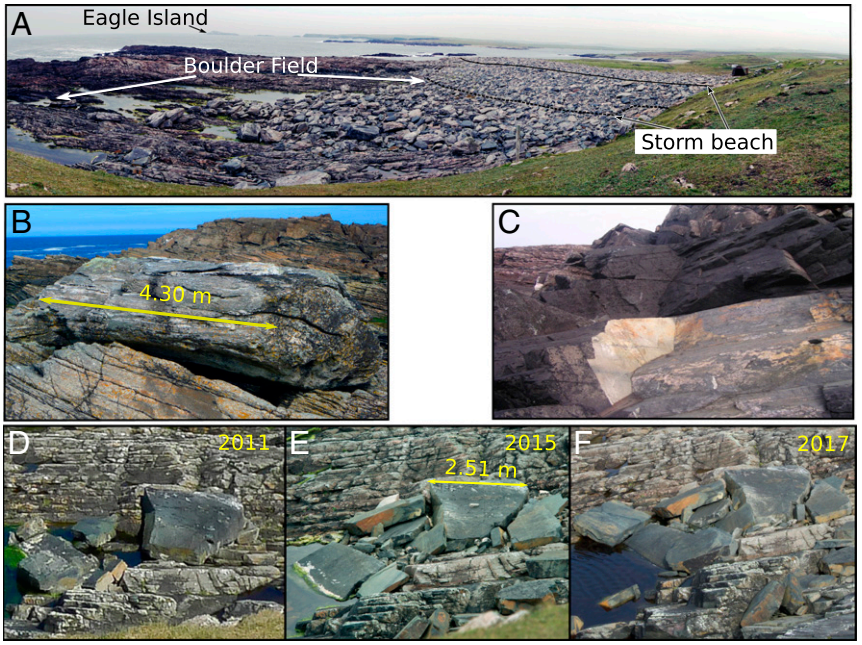

Fig. 2. (*A*) Panorama of the Annagh Head megaclast deposit taken from the ridge to the south, facing north. The approximate base of the storm beach is shown as a dotted line, and the crest is shown as a solid line. (*B*) The first megaclast to occur in the deposit, 115 m from the high tide line. (*C*) Pluck site located on small cliff to the south of the boulderite. (*D*) Photo of amphibolite boulders taken April 17, 2011. (*E*) Photo with field of view similar to *D* taken September 10, 2015 and (*F*) September 10, 2017. Location of photographs is 54°14′32.56″N, 10°6′21.73″W.

for each boulder: rock type; A (largest), B (intermediate), and C (shortest) dimensions of boulders; the degree of lichen coverage using an ordinal scale (0 for no lichen, 1 for sparse lichen, and 2 for significant lichen); the orientation of the upper surface; and the plunge of the longest axis.

All boulders are of locally derived gneiss (67%) or amphibolite (33%). Pluck sites (Fig. 2*C*) are visible in the cliff to the south of the wave-cut platform. The first boulder, weighing 48 tonnes, occurred 115 m from shoreline (Fig. 2*B*). The largest, weighing 53 tonnes, with no lichen coverage was 160 m from the shoreline. Boulder size reduced inshore, and the first gravel grains in the interstitial spaces between boulders occurred at 190 m (Fig. 1*C* and Table S2). A steep imbricated storm beach deposit whose toe occurs 195 m from the low tide mark has a bar crest length of 120 m and height of 9 m above mean high water, which is 100 m from the toe (Figs. 1 *C* and *D* and 2*A*). There is a logarithmic decrease in size with distance from the shoreline (Fig. 1*C*). The boulders are generally oblate (Fig. 3*B*), and many have no visible lichen on upper surfaces (Fig. 1*C*), suggesting that they have been plucked or rolled within recent decades. The long axes of boulders are generally aligned perpendicular to the dip of the storm beach (Fig. 1*D*).

Fig. 4 shows the minimum tsunami bore or storm wave heights required to pluck these joint-bounded boulders and to move them by sliding if subaerial. The hydrodynamic equations (18) and the parameters used are given in *Numerical Model* and indicate a value of 30 m for a storm wave and 7.5 m for a tsunami. A 7.5-m tsunami would pluck boulders and transport them more than 250 m inland (Fig. 3*A*). A 30-m-high storm wave with a period of 25 s is consistent with the distribution observed but could only pluck the largest boulders up to 100 m inland (Fig. 3*B*).

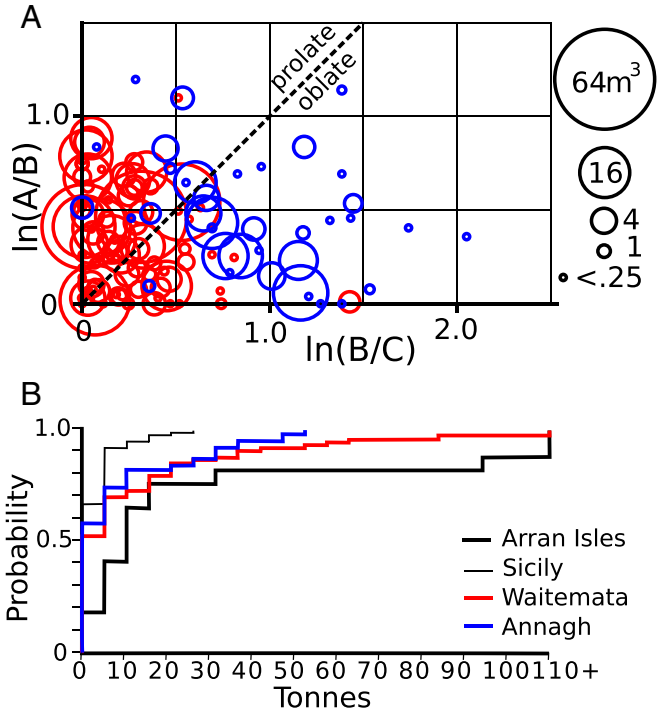

Fig. 3. (*A*) Plot showing the shape of the boulders from Waitemata (red) and Annagh Head (blue). The areas of the circles are proportional to the volume of the boulders. Note that the majority of Waitemata boulders fall in the prolate field, while those of the Annagh Head deposit fall in the oblate field. (*B*) Cumulative frequency distribution of boulders from the Waitemata Formation ($n = 86$) and Annagh Head ($n = 39$) compared with samples taken from the literature. Data for CTSDs from the Arran Isles, western Ireland (7), and from Sicily (17) are plotted for comparison purposes.

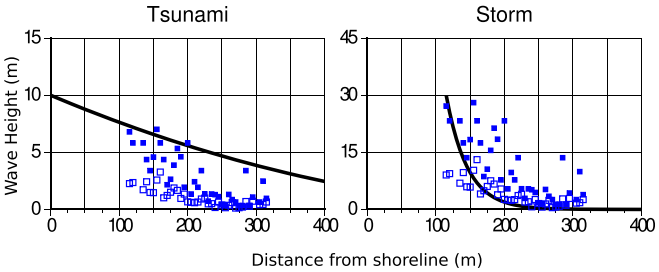

Fig. 4. The wave heights for either tsunami or storm waves required to pluck (filled symbol) or move (open symbol) the boulders on the Annagh Head traverse using the equations of Nandasena et al. (18) (squares) plotted against distance along the traverse, with zero distance at the shoreline. The heavy solid line on *A* represents the run-up heights for a 10-m tsunami with a period of 400 s, and the heavy solid line on *B* represents the run-up heights for a breaking 30-m wave with a period of 25 s that breaks at the position of the first boulder (19).

The site, 190 m inland and at a height of 5 m, was revisited on September 10, 2015, after the severe winter storms where 12 d of storm-force or greater winds were reported in the period December 5, 2013, to February 12, 2014 (20), and again on September 10, 2017. Photographs taken on those dates (Fig. 2 *D*–*F*) show that the deposit is continuously active, with new boulders of mass up to 5.2 tonnes being introduced.

These results are in good agreement with recent oceanographic data, models, and historical data. A wave buoy is located not far offshore: Wave Rider Belmullet Berth B (latitude, 54.2339; longitude, −10.1429; "Berth B", Fig. 1*B*). Data from this buoy, based upon 30-min observation periods, are publicly available from www.digitalocean.ie. Berth B has recorded four events since December 4, 2009, where significant wave height (H_s) exceeded 20 m, the largest from the northwest being 26.5 m (peak period 25 s) on January 15, 2015. During the winter storms of 2013/2014, Berth B recorded a significant wave height of 22.34 m (peak period 25 s) on January 27, 2014.

Assuming that these data are representative and conform to a Raleigh series distribution, the probability of a maximum wave height H_m for a given H_s can be estimated by the methodology given in *Numerical Model*. This suggests that 30-m-high waves will occur approximately 61 times in a 100-y period at Berth B. A similar approach using shorter-term, nearshore acoustic Doppler current profiler (ADCP) wave buoy observations (ref. 14 and Fig. 1*B*) forecasts ~15 waves of 20 m height per 100 y and a wave of 30 m in height every 500 y for a peak periods of 25.0 s.

Historical data for the Eagle Rock lighthouse some 4.8 km north of Annagh Head on a bearing of 013° (Figs. 1*B* and 2*A*) record seven extreme storm wave events since 1830 (12, 21) that damaged the lighthouse whose base is 59.7 m OD (ordnance datum). A storm wave in 1861 overtopped the tower at 67 m OD (21).

The Annagh Head deposit was described as a >4000 B.P. tsunami boulder deposit (7). This is based on a radiocarbon date for peat covering boulder deposits in the sheltered south side of the peninsula (Fig. 1*D*) and the maximum size of up to 40 tons reported for the boulders on the foreshore. This conclusion is disputed for Irish cliff-top boulderites, which are attributed to plucking and transport by storm waves (ref. 6 and references therein). Our field data indicate that the boulderite on the foreshore (Profile A-A′, Fig. 1*D*) is a CTSD in that the deposit between the shoreline and the active storm beach shows a rapid systematic decrease in size with distance from the shoreline, the storm beach does not lie stratigraphically on top of a separate megaclast deposit (rather one merges into the other) (Fig. 2*A*), the deposit is localized, the storm beach is active, and patterns of lichen coverage provide evidence that some megaclasts have

been rolled. Furthermore, historical and modeling data suggest that this area is subject to several waves of heights (20 m to 30 m) sufficient to pluck and move the megaclasts each century.

New Zealand

From Cape Rodney to Kawau Island, on the Pacific coast of the North Island of New Zealand about 80 km north of Auckland, the Lower Miocene, clastic, Waitemata Group is regionally subhorizontal and unconformable on the Permian to Jurassic Waipapa Group basement (22). The general stratigraphy of the Waitemata Group and its relationship with its Waipapa basement are shown in Fig. 5 (see *Waitemata Tectonic Background*). The lower part of the Waitemata Group and its unconformable contact with the Waipapa Group are superbly exposed on the rocky foreshore from Daniels Reef to south Matheson's Bay and may be divided (22) into a lower shallow marine sequence (Wawau Subgroup) with a maximum thickness of about 25 m on Kawau Island (Fig. 5*B*) and an upper mainly turbidite sequence (Warkworth Subgroup) derived from the northwest (23) with a minimum thickness of 1 km. The Warkworth Subgroup consists mainly of sandy turbidites and shales, containing slide masses, the volcaniclastic Parnell Grit, and flaggy bioturbated sandy limestones. Transgressive deposition of the Wawau Subgroup was across a complex rocky, irregular, shoreline of cliffs, sea stacks, and pinnacles with up to 200 m of relief, which was rapidly buried by Waitemata sediments, a sequence from littoral/neritic inner shelf sediments of the Wawau Subgroup (0 m to 200 m between Kawau Island and Cape Rodney) overlain by the deeper-water argillites/turbidites of the Warkworth Subgroup, which onlap without facies change onto basement, suggesting Wawau sea cliffs of at least 140 m. The Wawau coastline bears a strong resemblance to the present coastline; the Waitemata Group is being etched, resequently, from its Waipapa basement in small bays that coincide with small Wawau Bays, the best example being at Daniels Reef (Fig. 5*C*).

The lower part of the Wawau Subgroup (Fig. 5) consists of neritic and sublittoral sandstones, gritstones, and pebbly lithic sandstones, derived from the Waipapa (24), with an irregularly developed basal conglomerate of matrix-supported rounded/subrounded clasts of Waipapa rocks up to 1. 5 m across, some with *Pholad* borings and/or coral and *Lithothamnion* encrustations on their tops, reef corals in growth position, and rare abraded rhodoliths. The conglomerate blankets an irregular surface. Some herringbone structure in the basal sandstones suggests, at least in part, a littoral environment. Coarse neritic sandstones have both laminar and large-scale cross-bedded units with foresets dipping mainly northwest and are dominated by detritus with a Waipapa provenance; thin gray laminated siltstones are rare. As in the present-day shallow neritic sands of Cape Rodney, ray feeding excavations (*Piscichnus waitemata*) are very common in the lower Wawau Subgroup. The Wawau Subgroup contains a rich shallow marine fauna of mollusca, foraminifera, brachiopods, corals, cidarid echinoids, bryozoa, tube worms, ray feeding excavations, *Thalassinoides*, and inner shelf benthic foraminifera (25).

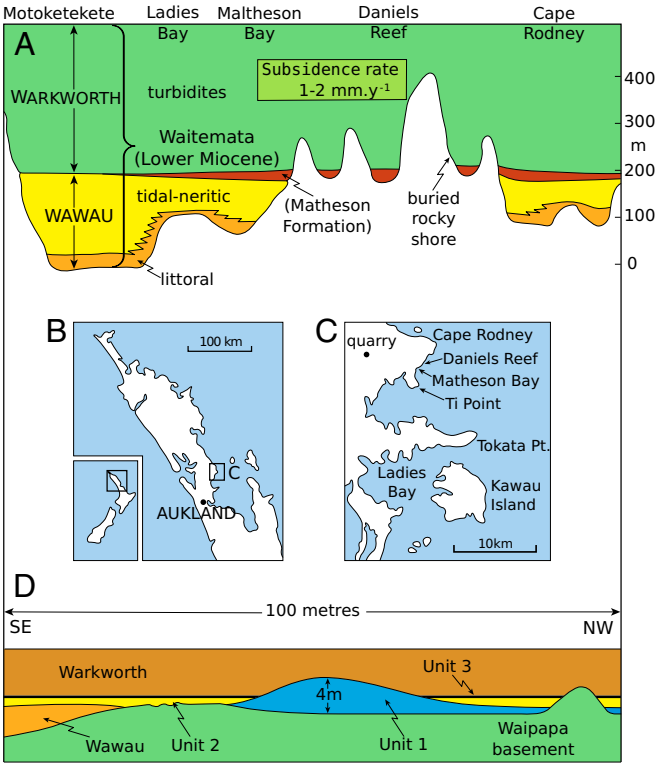

Fig. 5. (*A*) General stratigraphy of the Waitemata Group from Motuketekete Island to Cape Rodney. (*B*) General location map. (*C*) Map of the region showing localities mentioned in the text (*New Zealand*). (*D*) Schematic stratigraphy of the Matheson Formation at Matheson Bay. Tokata Pt., Tokata Point.

Matheson Formation

The thin upper part of the Wawau Subgroup, here termed the Matheson Formation (new term), is the focus of this section of the paper. The Matheson Formation has a complex stratigraphy, facies variation, and arrangement, varying from less than a meter to 4 m in thickness (Fig. 5). It overlaps the lower Wawau sediments northwestward onto Waipapa basement and consists, in sequence, of three main facies: (unit 1) a lower megaclast unit or Breccia Unit (22) with mainly angular to subangular boulders up to 143 tonnes (assuming a density of 2,700 $kg{\cdot}m^{-3}$) and fewer rounded to subrounded boulders commoner near the base (Fig. 6*C*); (unit 2) a medial coquina breccia unit (Fig. 6*G*), with a matrix of reworked lower Wawau sandstone, small subrounded to angular pebbles of Waipapa like those of the megaboulder unit, common rhodoliths (slow-growing, long-lived, nongeniculate coralline algae), commonly nucleated on small pebbles, and comminuted shell hash rich in bryozoa and molluscs (Fig. 6*H*), dominated by the large oyster *Crenostrea gittosina*, with lenses of the deep-water barnacle *Bathylasma aucklandicum* (Fig. 6*I*) and small pebbles at the top, and (unit 3) an upper thin gray buff-weathering siltstone lining depressions between boulder ridges (Fig. 6*J*). Matheson Formation nonorganic detritus was almost wholly derived from the Waipapa, with a very small volcaniclastic input. The three Matheson units vary greatly in thickness, and vertical and lateral arrangement; each unit may rest upon any lower unit including Waipapa basement (Fig. 5*D*). Because of the irregular thickness distribution of unit 1, unit 3 forms large flat-lying areas in depressions, the edges of which butt against all lower units.

Unit 1 shows substantial variation in thickness and character from half a meter of small boulders at Daniels reef (Fig. 6 *A* and *B*) to two and a half meters of breccia including megaboulders up to 143 tonnes at north Matheson Bay (Fig. 6 *C* and *J*). There is a clear difference between smaller rounded/subrounded boulders that are up to a few tonnes and angular boulders up to 143 tonnes (Fig. 3*A*). The rounded clasts were probably derived as boulders from the base of the Wawau, whereas the angular boulders were derived by catastrophic plucking from rock faces. No boulder in the coarsest unit, whether rounded or angular, has been seen to be bored or encrusted—the unit is chaotic (Fig. 6 *C–E*); there is no obvious tiling or imbrication. The matrix is a mixture of lithic sand of clear Waipapa ultimate origin, probably via the neritic/sublittoral Wawau, and comminuted shell hash. The matrix varies from almost wholly lithic, to wholly shell hash,

Fig. 6. (*A*) Daniels Reef. The flat-lying Matheson Formation rests upon an irregular contact with Waipapa basement of about 5 m relief. In the immediate foreground, Waipapa basement has a 1-m veneer of unit 1; in the near middle distance, 1 m of unit 2 is overlain by a thin cap of unit 3 yellow-brown siltstones on the far side of which the Matheson Formation abuts a basement ridge. (*B*) Reverse-graded unit 2 at Daniels Reef overlies unit 1. (*C*) Unit 1 megabreccia, north Matheson Bay, with megaclasts up to 120 tonnes. There is no imbrication or obvious fabric in the megabreccia. (*D*) Unit 1 megabreccia with small subrounded and larger angular clasts, south Matheson Bay. (*E*) Unit 1 with small megaclasts in yellow lithic and shell hash matrix, north Matheson Bay. (*F*) Unit 1, north Matheson Bay, with rounded, subrounded, and angular boulders, showing fragmentation and shell hash injection. (*G*) Irregular contact with about a meter of relief between basement and unit 2 coquina, and subrounded boulders at base of coqina, south Matheson Bay. (*H*) Unit 1, north Matheson Bay, breccia with mixed lithic sand, shell hash, and shell matrix. (*I*) Unit 1, north Matheson Bay, *Bathylasma* lens. (*J*) Unit 3 siltstone in depression butting against unit 1 megabreccia.

to pebbly coquina. Jointing in the Waipapa probably controlled the detachment or plucking of massive fine-grained greywacke boulders, whereas strongly foliated Waipapa greywacke and argillite boulders shapes were controlled by foliation. Angular and subangular boulders dominate at all sizes. Unit 1 is very similar to a Plio-Pleistocene tsunamite at Horritos in northern Chile, where angular to subangular boulders of basement up to 5 tons have a matrix of comminuted shell-rich sand (26). On the southeast side of the rocky foreshore at north Matheson Bay, unit 3 siltstones butt against a sandstone sequence that may be Wawau redeposited as small-scale chevrons (23, 22); these sandstones have a bedding sheeting resembling giant current bedding dipping gently northwestward.

Boulder dimensions were measured for 89 randomly selected boulders distributed over the whole outcrop. The majority of the boulders are prolate in shape (Fig. 3*B*). The height of a tsunami required to pluck these boulders is estimated at 12.0 m to 13.0 m (Fig. 7). The height of a tsunami wave required to move these boulders by sliding is similarly estimated at around 2 m or less (Fig. 7). This implies (27) that the run-up distance for such a tsunami was perhaps between 580 m (period of 400 s) and 5,220 m (period of 3,600 s). The distance from the paleo shoreline at Matheson Bay to the westernmost (inland) Omaha Valley Quarry exposure of the Matheson Formation is 5.8 km.

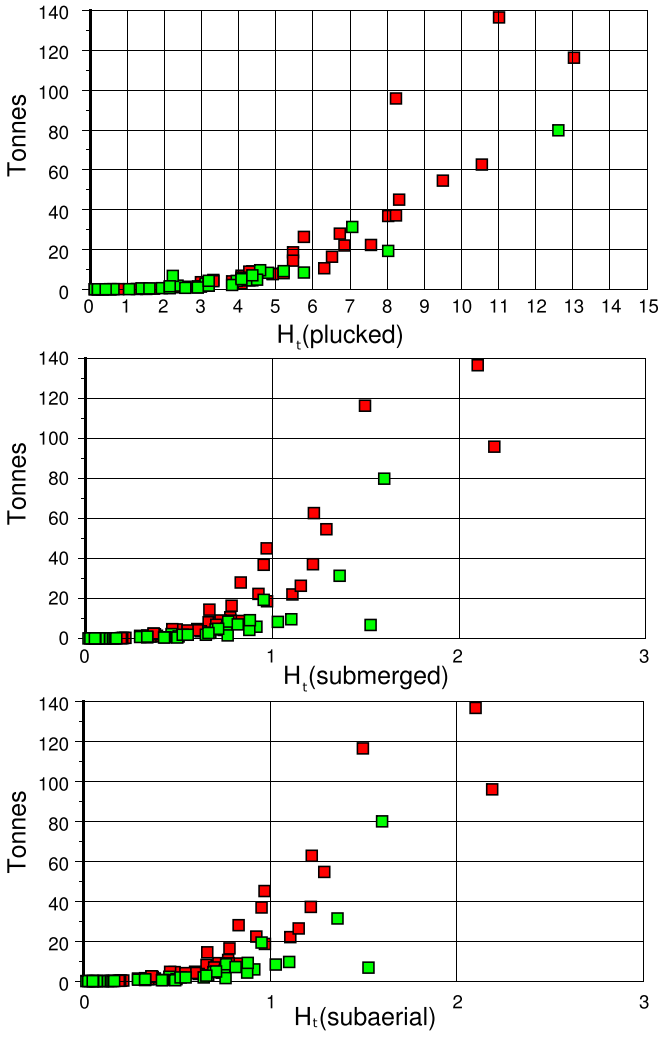

Fig. 7. The estimated maximum tsunami wave heights required to pluck [H_t (plucked)] the boulders in the Matheson Formation and the tsunami heights required to move submerged boulders [H_t, (submerged)] and subaerial [H_t (subaerial)] boulders by sliding using the equations Nandasena et al. (18) (squares). Prolate boulders are shown in red and oblate in green.

Therefore, we suggest that this tsunami had a period on the order of 1 h.

The megabreccias were interpreted as deposited by neritic/littoral processes involving gravity slides from local cliffs (22). We suggest, alternatively, that the Matheson Formation was deposited during a very short-lived pal-event, geologically instantaneously, by a tsunami surge and retreat. It is unlikely that the Matheson pal-event was related to a storm surge or freak wave, mainly because of its 80-km coastal distribution from Cape Rodney to Mototapu Island just North of Auckland. Its presence in the Omaha Valley Quarry some 5 km inland from the Miocene rocky shoreline also suggests a tsunami run-up. Consistent with a tsunami origin, there is clear evidence of impact, crushing, and vein fragmentation of boulders, with the injection of matrix into veins (Fig. 6*F*). On the basement ridge south of Daniels Reef, cracks in basement are filled to several meters with a fine shell hash, suggesting hydraulic injection. Transport of the boulders and matrix was, therefore, probably simultaneous, indicating bed-load transport in sediment slurry. We think it likely that the rounded boulders were derived from the littoral boulder facies, whereas the angular boulders were formed by hydraulic plucking. Large tsunamis commonly cause substantial instantaneous denudation of bedrock, including fluting, grooving, and plucking (28). Although the Waipapa surface is highly irregular at all scales, there is too little areal exposure of the surface to make such observations. We suggest that the megaboulder unit 1 was deposited by a tsunami with a northwestward run-up of at least 5 km and that unit 2 with its common reverse grading (Fig. 6*B*) was the backwash deposit. At north Matheson Bay, unit 2 shows a rapid but smooth lateral grading from a rhodolith and oyster-rich facies southeastward to a finer-grained rhodolith-free facies.

The apparent paradox of mixed shallow and deep-water marine faunas in the Matheson Formation, both macro and micro, was attributed to slumping of shallow water sediments and fauna into a bathyal mixing zone (22). We think that this is unlikely, because the Matheson Formation rests conformably on the sublittoral Wawau. Faunal mixing is consistent with a tsunami run-up bringing deeper water faunas up into the littoral/sublittoral environment. We suggest that the *Bathylasma* plate horizon at the top of the reverse-graded unit 2 was the final deposit of the backwash, overlain by the immediately posttsunami unit 3 silt. Ricketts et al. (22) also mused on the very thin sequence (Matheson Bay Formation) that effects the transition from the shallow marine Wawau Subgroup to the bathyal Warkworth turbidites and considered the deepening to have taken place in less than 1 My. The Matheson Formation clearly lies at a critical tectono-stratigraphic rapid transition from the Wawau neritic sediments (to 100 m) to the increasingly bathyal Warkworth turbidites (1,700 m). We suggest that this may have been the result of rapid flexural loading by the advancing Northland Ophiolite Allochthon and that a submarine, obduction-related, major earthquake caused the tsunami. Our conclusion is that the Matheson Formation was deposited by a tsunami and backwash, and that the run-up reached at least 5 km inland to the position of the present-day Matakana quarry, a present elevation difference of about 30 m. The early Wawau coastal topography was not slowly buried by a gradually rising sea level but was engulfed during extremely rapid subsidence of the Waitemata Basin to 1,700 m at a rate of 1 mm·y^{-1} to 2 mm·y^{-1} (22); 200 m of relief would have been inundated in 100,000 y to 200,000 y. The Matheson Formation marks the onset of this period of rapid subsidence and was deposited geologically instantaneously as a time–rock marker, not as a result of peaceful coastal sedimentation with complex littoral to sublittoral facies changes as was previously attributed.

Numerical Modeling

Although we are confident that the field relationships suggest the Matheson Formation was deposited by a tsunami or a sequence of tsunamis, the origin of the megaclast deposits at Annagh Head is disputed (6–8). We test the conclusion that the Annagh Head deposit is a CTSD by using a numerical model, based on local oceanographic real-time data, which tests whether such large boulders could be plucked and moved by Atlantic storm waves. The model first uses a Monte Carlo experiment to construct wave catalogs (Fig. 8*A*) from the Berth B buoy and the Ballyglass Tide gauge data. Each wave is then tested to see whether it could pluck a boulder of a minimum mass and defined shape (or whether the boulder was already plucked) and move the boulder up the platform (Fig. 8 *B* and *C*). The details of the method used are given in *Numerical Model*.

Plucking and Boulder Shape

The boulderites in the Matheson Formation are dominantly of prolate form, and those from Annagh Head are of oblate form, suggesting that boulder shape might be a significant factor in the

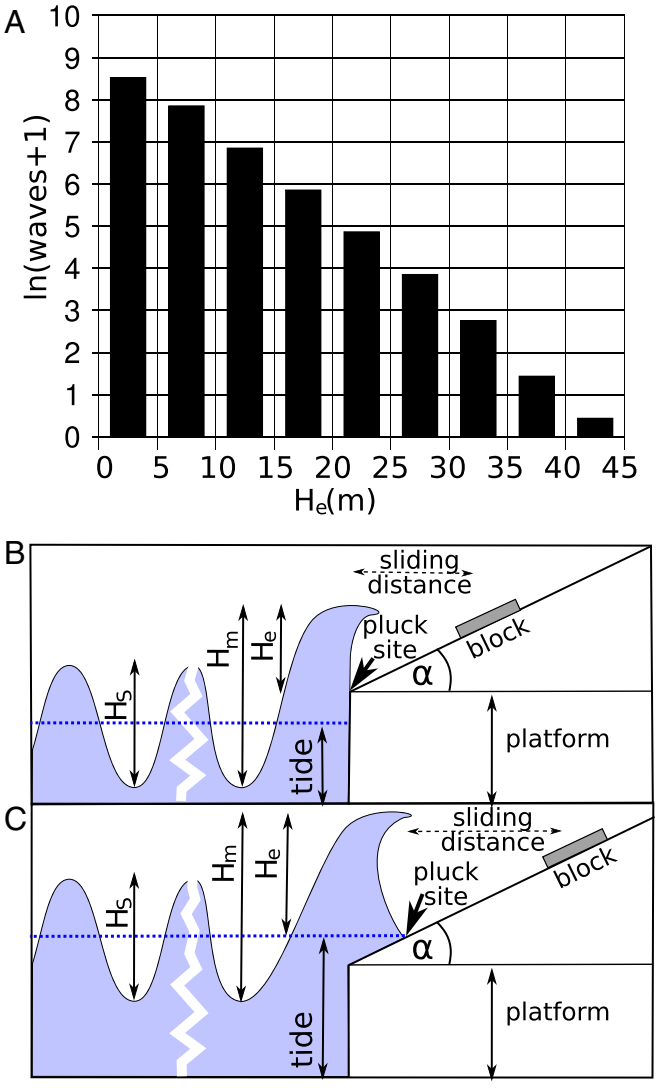

Fig. 8. (*A*) Histogram showing wave heights (logarithmic scale) computed for one 5-y segment of a model run. The model space used for the numerical model where (*B*) the tide was below the rocky platform and (*C*) the tide was at or above the rocky platform. See *Numerical Model* for details.

formation of boulderites. We investigate the effect of boulder shape on the size and number of boulders that could be plucked each year in this region, using 50 independently generated 5-y wave catalogs. The number of boulders and mass of the largest boulder plucked in a year for various boulder shapes and hydrodynamic equations (18, 29) at the cliff top of a 4-m-high platform that slopes at 1° were computed. Oblate, prolate, and cubic boulder shapes were used in the models, and only boulders above 8 m^3 were considered. The results (Fig. 9) predict that more, larger boulders with a bias toward oblate shape should be plucked. It is important to note that, given this wave catalog, both hydrodynamic equations predict that boulders of tens of tonnes can be plucked.

Modeling a Cliff-Top Storm Deposit

A similar 250-y wave catalog was used to test the effects on both plucking and sliding of boulders on a 2-m-high platform that sloped at 1°. Only boulders larger than 11 m^3 were considered. To control for shape, all boulders were given the mean values for A/B = 1.6 and B/C = 2.4 observed at Annagh Head.

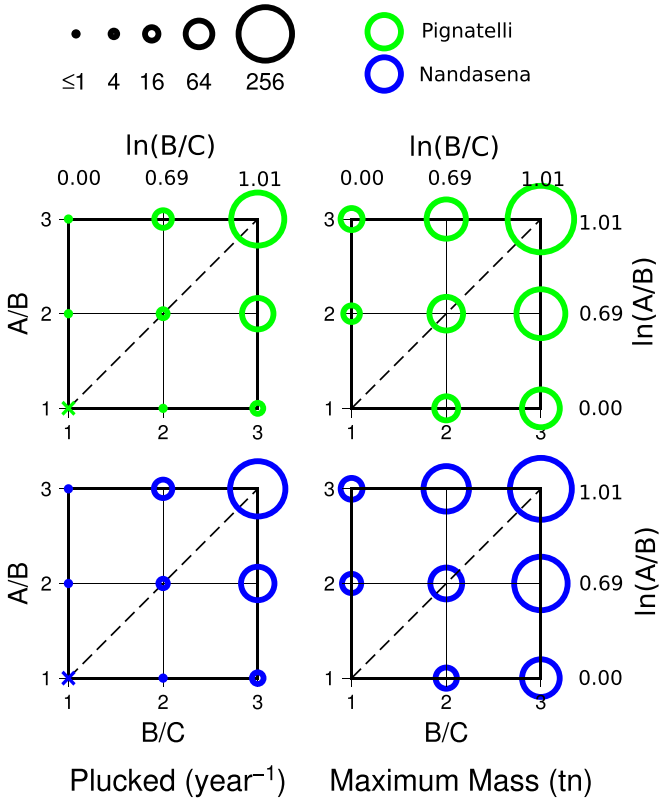

Fig. 9. The effects of boulder shape on plucking of joint-sided boulders using the hydrodynamic equations of Pignatelli et al. (29) (green) and Nandasena et al. (18) (blue). Shown are the average number of boulders plucked per year (*Left*) and the maximum weights of the largest boulders plucked (*Right*) . The areas of the circles correspond to the magnitude of the result; a diagonal cross indicates no boulder plucked. The model run parameters were as follows: Wave heights were estimated from the Wave Rider Belmullet Berth B Buoy and the Ballyglass tide gauge for the years 2011–2015; platform height = 4.0 m; minimum boulder volume = 8 m^3; dip of the platform = 1°; specific gravity of rock = 2,775 kg·m^{-3} and sea water = 1,025 kg·m^{-3}; minimum and maximum azimuths of waves counted was 270° to 320°; number of Monte Carlo experiments = 50. The diagonal dashed line represents $K = 1$ and separates the fields for prolate boulders $K > 1$ (*Top Left*) from that of oblate boulders $K < 1$ (*Bottom Right*). See *Plucking and Boulder Shape* for details.

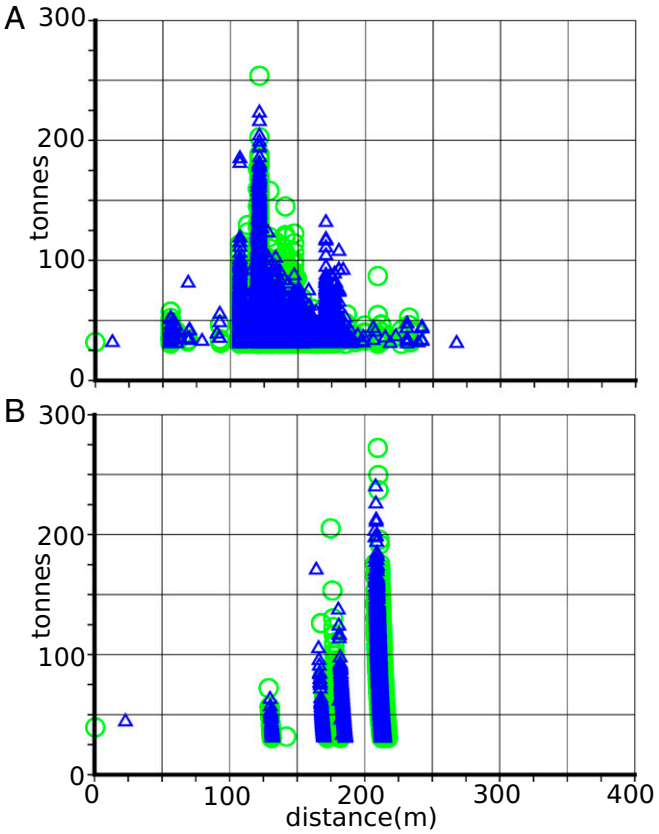

Fig. 10. (*A*) Results of model runs using the median shape of the Annagh Head boulders for a platforms of 2 m height. The run parameters were as for Fig. 9, except the boulder shape was fixed at P = A/B = 1.6 and q = B/C = 2.4, which were the median values for the Annagh Head boulders > 20 tonnes, and the minimum boulder size was set at 11 m^3, equivalent to 30.5 tonnes, to minimize computation. Wave run-up was modeled as that of (*A*) a breaking wave (19) and (*B*) a bore (27). Analysis based on the equations of Nandasena et al. (ref. 18, blue triangles) and Pignatelli et al. (ref. 29, green circles). See *Numerical Model* for method.

A significant CTSD is generated, where the model uses the equations of Nandasena et al. (18) or Pignatelli et al. (29) to assess the dimensions of a plucked boulder. A model based on the Nott (30) equations plucked only two boulders of this shape. The model produces CTSDs (Fig. 10*A*) that are similar to that at Annagh Head where the run-up is based on that of a breaking wave (20). A zone, extending from the cliff edge to 105 m, is relatively free of boulders. The main deposit is then predicted from this point to 240 m, decreasing in size and frequency inland. The boulderite deposit of Annagh Head extends from 115 m to 200 m, with a decrease in maximum size inland (Fig. 1*C*). A model (Fig. 10*B*), assuming that the run-up can be modeled as a bore (27), predicted that the main boulderite deposit would be at a distance of 220 m from the cliff edge.

Field observations differ from the model. The maximum predicted boulder size, based on the equations of Nandasena et al. (18) or Pignatelli et al. (29), is approximately 4 times larger than that observed, and the volume of the boulders plucked exceeds the combined volume of the boulderite deposit and storm beach by a factor of 13 to 15 (Table 1). However, the model assumes that each wave will pluck the largest possible boulder. In reality, the pluck site must have suitably spaced, open joints for this to happen, and this depends upon local geology and weathering rates. It is, therefore, inevitable that such a model will overestimate both the volume and frequency of boulders entrained into the deposit.

Table 1. Model versus field data for Annagh Head

Field data	Model 1 (Nandasena)	Model 2 (Pignatelli)	Model 3 (Nott)	Run (duration)
Maximum mass, tonnes				
53.0	240.1	272.3	35.5	1 (250 y)
	222.9	253.9	34.1	2 (250 y)
Mean mass of blocks in the boulderite, tonnes				
23.8	42.5	42.3	34.5	1 (250 y)
	42.5	42.2	32.3	2 (250 y)
Volume of CTSD, m^3				
10,400 (boulderite)	1,178,835	1,040,340	25	1 (250 y)
70,200 (storm beach)	1,173,682	1,036,237	23	2 (250 y)

Model 1 used the equation of Nandasena et al. (20); model 2 used that of Pignatelli et al. (31), and model 3 used that of Nott (19) to assess the size of a boulder plucked by any given wave. Run 1 created the plots in Fig. 10A, and run 2 created the plots in Fig. 10B.

The large number of boulders that, potentially, could be plucked indicates that this process is a result neither of a few rogue waves nor of rogue observations in the dataset.

We believe that this model confirms that the real-time oceanographic data are consistent with the Annagh Head boulderite being a cliff-top storm deposit. However, a cautionary observation is that, if the Nott (30) equations are appropriate, the deposit, given the shape of the boulders, would probably have taken perhaps 3,350 y to accumulate. Also the treatment of the wave data from Buoy B as deep water wave data will likely lead to an overestimate of the breaking wave height, although the computed wave catalog (Fig. 8*A*) shows H_m significantly less than that for the observed storm waves at Eagle Island.

Discussion

The Annagh Head deposit, we suggest, is the result of local factors: the height of the storm waves, the presence of pluck sites on the cliff top with joint spacing that produces oblate boulders, and local topography. Our modeling shows that storm waves can produce a clear zone at the cliff edge and extreme boulder sizes (>100 tonnes), features characteristic of CTSDs (31). The boulderite stratigraphy at Annagh Head is complex, and our conclusions only refer to the active deposits. The origin of the peat-covered >4000 B.P. deposits (7) remains uncertain.

A key difference between tsunamite boulderites and storm-wave boulderites is that tsunamites carry a large percentage of suspended sediment, whereas storm waves do not. The matrix of Matheson Formation unit 1 is a grit/shell hash mixture, which was clearly syndepositional with the boulders. This indicates both very rapid (convulsive) deposition and that the fluid carrying the boulders was very viscous with suspended sediment, which greatly enhanced its carrying capacity compared with water, allowing the transport of much larger boulders. Other features that characterize CTSDs include the localized linear nature of the deposit (Figs. 1 and 2 and Table 2) confined to within a few hundred meters of the cliff line, local variability depending on coastline geomorphology (Fig. 1*D*), the presence of a cliff-top scour zone (Figs. 2*A* and 7), and imbrication (Fig. 1*D*). Features that characterize a tsunamite include evidence for a single pal-event (Fig. 5*A*) and aerially extensive deposits (Fig. 5*C*). Maximum size and size distribution are not necessarily discriminating factors (Fig. 3*B*). Our analysis suggests that the Matheson Formation may have

Table 2. A comparison of the boulderites at Annagh Head, County Mayo, Ireland, and the Lower Miocene Matheson Formation, New Zealand

Feature	Annagh Head	Matheson Formation
Dimensions of deposit	Boulder field deposit localized (120 m × 180 m) and grades into active storm beach	Deposit extensive 80,000 × 5,800 m (minimum area ~230 km^2 if triangular, ~460 km^2 if rectangular)
Maximum boulder size	53 tonnes	143 tonnes
Boulder source	Locally derived from cliff face	Locally derived from several depths
Matrix	Boulderites have no matrix, storm beach does	Shell hash matrix
Onshore–offshore relationships	Cliff-top wave scour zone of 115 m	Both submarine and subaerial, 4-m-high boulderite ridge (unit 2) narrow (15 m) littoral zone clear of blocks
Boulder shape (Fig. 3*B*)	Dominantly oblate: mostly angular	Dominantly prolate: angular and rounded
Imbrication	Imbrication both in boulderite and storm beach deposits	No tiling or imbrication, because few oblate, slab-like, boulders
No. of events	Field evidence for repeat events supported by modeling	Evidence of single pal-event
Boulder ridge	Largest boulders deposited on rocky platform, smaller boulders < 3 m^3 form ridge	Largest boulders form ridge
Boulder preservation	Angular fracturing of boulders during recent storms, no matrix injection	Cracking of boulders with matrix injection
Boulder orientation	Long axes of oblate boulders roughly parallel with shoreline	Long axes of prolate boulders roughly parallel with paleo-shoreline
Size distribution (Fig. 3*A*; note that sampling for Annagh Head was for the largest boulder)	57% less than 5 tonnes	52% less than 5 tonnes

been deposited in 1 h, while the CTSD at Annagh Head has developed over centuries. The abundance of oblate boulders in the Annagh Head deposit (Fig. 3 and Table S3) and the results of our modeling which shows more and larger oblate boulders may be included in a CTSD for a given wave catalog (Fig. 9) both suggest that boulder shape is a useful area for future research into discriminating between tsunamites and CTSDs.

Conclusions

The properties of these two boulderites are summarized in Fig. 3 and Table 2. We believe that a single pal-event tsunami origin for the Matheson Formation is consistent with its geographical extent (>200 km^2); the ubiquitous presence of a shelly matrix that is locally injected into fractured boulders; and the presence of rounded, abraded boulders. Arguments for the Annagh Head boulderite being a cliff-top storm deposit include its limited and localized geographic extent (0.006 km^2), the lack of matrix in much of the boulderite deposit, the boulderite deposit grading into an active storm beach on its lee side, the presence of a shoreward zone of 115 m scoured of boulders, and field evidence for the movement of boulders during recent storms. Modeling, based on real-time oceanographic data, is consistent with this conclusion, at least for the boulderite field along the section A-A′ (Fig. 1*D*).

ACKNOWLEDGMENTS. We thank Mike Isaac, Rick Sibson, and Julie Rowland for sharing their knowledge and understanding of New Zealand geology, and Martin White for oceanographic advice.

1. Ager D (1981) *The Nature of the Stratigraphical Record* (John Wiley, New York).
2. Ager D, Ager DV (1995) *The New Catastrophism* (Cambridge Univ Press, Cambridge, UK).
3. Hallam A (2005) *Catastrophes and Lesser Calamities: The Causes of Mass Extinctions* (Oxford Univ Press, Oxford).
4. Williams DM, Hall AM (2004) Cliff-top megaclast deposits of Ireland, a record of extreme waves in the North Atlantic—Storms or tsunamis? *Mar Geol* 206:101–117.
5. Cox R, Zentner DB, Kirchner BJ, Cook MS (2012) Boulder ridges on the Aran Islands (Ireland): Recent movements caused by storm waves, not tsunamis. *J Geol* 120: 249–272.
6. Hall AM, Hansom JD, Williams DM (2010) Wave-emplaced coarse debris and megaclasts in Ireland and Scotland: Boulder transport in a high-energy littoral environment: A discussion. *J Geol* 118:699–704.
7. Scheffers A, Scheffers S, Kelletat D, Browne T (2009) Wave-emplaced coarse debris and megaclasts in Ireland and Scotland: Boulder transport in a high-energy littoral environment. *J Geol* 117:553–573.
8. Scheffers A, Kelletat D, Scheffers S (2010) Wave-emplaced coarse debris and megaclasts in Ireland and Scotland: Boulder transport in a high-energy littoral environment: A reply. *J Geol* 118:705–709.
9. Johnson ME (1988) Why are ancient rocky shore lines so uncommon? *J Geol* 96: 469–480.
10. Terry JP, Goff J (2014) Megaclasts: Proposed revised nomenclature at the coarse end of the Udden-Wentworth grain-size scale for sedimentary particles. *J Sediment Res* 84:192–197.
11. Dublin Institute of Advanced Studies (2017) Irish National Seismic Network. Available at https://www.insn.ie/. Accessed March 28, 2017.
12. O'Brien L, Dudley JM, Dias F (2013) Extreme wave events in Ireland: 14,680 BP-2012. *Nat Hazards Earth Syst Sci* 13:625–648.
13. INFOMAR (2016) *Broadhaven Bay Bathymetric Contour Chart 1:50,000* (Integ Mapping Sustainable Dev Ireland's Mar Resour, Dublin).
14. Cahill BG, Lewis T (2013) Wave energy resource characterisation of the Atlantic Marine Energy Test Site. *Int J Mar Energy* 1:3–15.
15. Menuge J, Daly JS (1994) The Annagh Gneiss complex in County Mayo, Ireland. *A Revised Correlation of Precambrian Rocks in the British Isles* (Geol Soc Spec Pub, London), Vol 22, pp 59–62.
16. Winchester JA, Max MD (1987) The pre-Caledonian Inishkea Division of northwest Co. Mayo, Ireland: Its chemistry and probable stratigraphic position. *Geol J* 22:309–331.
17. Barbano MS, Pirrotta C, Gerardi F (2010) Large boulders along the south-eastern Ionian coast of Sicily: Storm or tsunami deposits? *Mar Geol* 275:140–154.
18. Nandasena NAK, Paris R, Tanaka N (2011) Reassessment of hydrodynamic equations: Minimum flow velocity to initiate boulder transport by high energy events (storms, tsunamis). *Mar Geol* 281:70–84.
19. Sunamura T (1985) A simple relationship for predicting wave height in the surf zone with a uniformly sloping bottom. *Trans Jpn Geomorphol Union* 6:361–364.
20. Met Éireann (2017) *Winter 2013/2014*. Available at www.met.ie/climate-ireland/weather-events/WinterStorms13_14.pdf. Accessed January 24, 2017.
21. Commissioner for Irish Lights (CIL) (2017) *Eagle Island Lighthouse*. Available at www.irishlights.ie/tourism/our-lighthouses/eagle-island.aspx. Accessed January 24 2017.
22. Ricketts BD, Ballance PF, Hayward BW, Mayer W (1989) Basal Waitemata Group lithofacies: Rapid subsidence in an early Miocene interarc basin, New Zealand. *Sedimentology* 36:559–580.
23. Gregory MR (1969) Sedimentary features and penecontemporaneous slumping in the Waitemata Group, Whangaparaoa Peninsula, North Auckland, New Zealand. *N Z J Geol Geophys* 12:248–282.
24. Hayward BW, Smale D (1992) Heavy minerals and the provenance history of Waitemata Basin Sediments (early Miocene, Northland, New Zealand). *N Z J Geol Geophys* 35:223–242.
25. Eagle MK, Hayward BW, Grant-Mackie JA, Gregory MR (1999) Fossil communities in an early Miocene transgressive sequence, Mathesons Bay, Leigh, Auckland. *Tane* 37: 43–67.
26. Hartley A, Howell J, Mather AE, Chong G (2001) A possible Plio-Pleistocene tsunami deposit, Hornitos, northern Chile. *Rev Geol Chile* 28:1–9.
27. Noormets R, Crook KA, Felton EA (2004) Sedimentology of rocky shorelines: 3. Hydrodynamics of megaclast emplacement and transport on a shore platform, Oahu, Hawaii. *Sediment Geol* 172:41–65.
28. Bryant EA, Young RW (1996) Bedrock-sculpturing by tsunami, south coast New South Wales, Australia. *J Geol* 104:565–582.
29. Pignatelli C, Sansò P, Mastronuzzi G (2009) Evaluation of tsunami flooding using geomorphologic evidence. *Mar Geol* 260:6–18.
30. Nott J (2003) Waves, coastal boulder deposits and the importance of the pre-transport setting. *Earth Planet Sci Lett* 210:269–276.
31. Kennedy AB, et al. (2017) Extreme block and boulder transport along a cliffed coastline (Calicoan Island, Philippines) during Super Typhoon Haiyan. *Mar Geol* 383: 65–77.
32. Bryant EA, Nott J (2001) Geological indicators of large tsunami in Australia. *Nat Hazards* 24:231–249.
33. Goff J, Weiss W, Courtney C, Dominey-Howes D (2010) Testing the hypothesis for tsunami boulder deposition from suspension. *Mar Geol* 277:73–77.
34. Ramalho RS, et al. (2015) Hazard potential of volcanic flank collapses raised by new megatsunami evidence. *Sci Adv* 1:e1500546.
35. Mattoli GS, et al. (2007) Unique and remarkable dilatometer measurements of pyroclastic flow-generated tsunamis. *Geology* 35:25–28.
36. McMurtry GM, et al. (2004) Megatsunami deposits on Kohala volcano, Hawaii, from flank collapse of Mauna Loa. *Geology* 32:741–744.
37. Scheffers A, Kelletat D (2003) Sedimentologic and geomorphologic tsunami imprints worldwide—A review. *Earth Sci Rev* 63:83–92.
38. Whelan F, Kelletat D (2002) Geomorphic evidence and relative and absolute dating results for tsunami events on Cyprus. *Sci Tsunami Hazards* 20:3–18.
39. Boulton SJ, Whitworth MRZ (2017) Block and boulder accumulations on the southern cost of Crete (Greece): Evidence for the 365 CE tsunami in the Eastern Mediterranean. *Geol Soc Spec Pub* 456:SP456.4.
40. Frohlich C, et al. (2009) Huge erratic boulders in Tonga deposited by a prehistoric tsunami. *Geology* 37:131–134.
41. Simkin T, Fisk RS (1983) *Krakatau 1883—The Volcanic Eruption and Its Effects* (Smithson Inst Press, Washington, DC).
42. Dewey JF, Taylor TR, Monastero FC (2008) Transtension in the brittle field: The Coso region, southern California. *Int Geol Rev* 50:193–217.
43. Ichinose GE, Anderson JG, Satake K, Schweickert RA, Lahren MM (2000) The potential hazard from tsunami and seiche waves generated by large earthquakes with Lake Tahoe, California-Nevada. *Geophys Res Lett* 27:1203–1206.
44. Moore JG, Schweickert RA, Robinson JE, Lahren MM, Kitts CA (2006) Tsunami-generated boulder ridges in Lake Tahoe, California-Nevada. *Geology* 34:965–968.
45. Melosh HJ (1987) The mechanics of large rock avalanches. *Rev Eng Geol* 7:41–50.
46. Bretz JH (1925) The Spokane flood beyond the channeled scablands. *J Geol* 33:97–115.
47. Plafker G, Ericksen GE, Concha JF (1971) Geological aspects of the May 31, 1970, Peru earthquake. *Bull Seismol Soc Am* 61:543–578.
48. Carrivick JL, Rushmer L (2006) Understanding high magnitude outburst floods. *Geol Today* 22:60–65.
49. Ballance PF (1974) An inter-arc flysch basin in northern New Zealand: Waitemata Group (Upper Oligocene to Lower Miocene). *J Geol* 82:438–471.
50. Hayward BW (1979) Eruptive history of the early to mid Miocene Waitakere volcanic arc, and palaeogeography of the Waitemata Basin, northern New Zealand. *J R Soc N Z* 9:297–320.
51. Isaac MJ, Herzer RH, Brook FJ, Hayward BW (1994) *Cretaceous and Cenozoic Sedimentary Basins of Northland, New Zealand*, Science Monograph (Inst Geol Nuclear Sci, Lower Hutt, New Zealand), Vol 8.
52. Sporli KB, Rowland JV (2007) Superposed deformation in turbidites and syn-sedimentary slides of the tectonically active Miocene Waitemata Basin, northern New Zealand. *Basin Res* 19:199–216.